Integrated Balanced BPSK and QPSK Modulators for the *Ka*-Band

HIROYO OGAWA, MASAYOSHI AIKAWA, MEMBER, IEEE, AND MASAMI AKAIKE, MEMBER, IEEE

Abstract—Microwave integrated circuit (MIC) balanced biphase-shift-keying (BPSK) and quadri-phase-shift-keying (QPSK) modulators have been achieved in the 27-GHz band. The modulators are fabricated using a combination of microstrip lines and slot lines, viz., tow-sided MIC. The diodes used are beam-lean Schottky-barrier diodes. Balanced BPSK modulation is performed by path-switching and mode transformation from the slot line to microstrip lines. The insertion loss is 2.2 dB at a carrier frequency of 27 GHz. The phase error and the amplitude deviation are less than 1° and 0.5 dB, respectively.

The QPSK modulator consists of two BPSK modulators, a power divider, and a branch-line hybrid coupler. The configuration of the modulator is the parallel-connected type. The insertion loss is 6.3 dB at a carrier frequency of 27 GHz. The phase error is less than 2°, and the rise time and fall time of the modulated carrier are less than 300 ps. The isolation between the carrier input port and the QPSK modulated carrier output port is greater than 25 dB. These modulators can be extended to the millimeter-wave band.

I. Introduction

RECENTLY, MICROWAVE integrated circuit (MIC) phase-shift-keying (PSK) modulators have been fabricated for use in digital communications [1]–[5]. PSK modulators are divided into two different types. The first is a balanced or a double-balanced type, and the second is a path-length modulator (unbalanced) type. Balanced modulators have been realized as ring or star modulators at microwave bands [6]–[8]. By using a combination of microstrip lines, slot lines, and coplanar lines, high bit-rate double-balanced modulators for BPSK have been realized at the *C*-band [1], [2], [9].

Path length modulators have been realized as reflection- or transmission-type modulators. The reflection-type modulators have been constructed by using a waveguide circulator [10], [11] or an MIC 3-dB branch-line hybrid coupler [12], [13]. The transmission-type modulators use two microstrip lines with different line lengths and two switching diodes [3]. In the path-length modulator, some amplitude variations and jitter occur in PSK waveforms due to the path-length difference. On the other hand, the balanced modulator using equal path lengths realizes PSK waveforms without jitter, in principle, and achieves good isolation between the carrier input port and the modulated carrier output port, and a good PSK waveform in a wide frequency band. Furthermore, the balanced modulator can be easily fabricated by the MIC technique, and is suitable for MIC construction because no circulators are required.

This paper first discusses a new BPSK balanced modulator which is proposed for use in the *Ka*-band. The modulator utilizes a combination of microstrip lines and slot lines (two-sided MIC).[1] The modulator consists of two quarter-wavelength slot lines, two switching diodes, a slot-to-microstrip transition, and a gold (Au) wire. The modulator proposed in this paper has the following advantages:

1) high isolation between the carrier input port and the modulated carrier output port is obtained due to the balanced configuration;
2) pulsewidth variations and amplitude deviations are suppressed due to the balanced configuration;
3) for a baseband input circuit, a simple configuration achieved with only a wire bonding is sufficient;
4) it is suitable for high frequency bands up to the millimeter-wave band;
5) a dc return path is not required because slot lines are used.

The latter part of this paper will be devoted to a discussion of the QPSK modulators which can be made by combining two BPSK modulators in series or in parallel [14], [15]. In this paper, a parallel-connected balanced QPSK modulator using two BPSK modulators is presented. This modulator showed good performance, and can be extended to the millimeter-wave band.

II. BPSK Balanced Modulator

A. Circuit Configuration

The configuration of a BPSK balanced modulator is shown in Fig. 1. The dimensions of the circuit pattern are also described. The modulator is composed of slotlines, microstrip lines, a gold (Au) wire, and two beam-lead Schottky-barrier diodes. In this figure, solid lines indicate microstrip lines on the substrate, while dotted lines indicate slotlines on the reverse side of the substrate. The carrier input port, the BPSK modulated carrier output port, and the modulating pulse input port are denoted by *C*, *M*, and *P*, respectively. The Au wire is used to supply modulating pulses to the diodes.

The balanced modulator previously reported [9] used

Manuscript received July 10, 1981; revised October 20, 1981.

The authors are with the Radio Transmission Section, Yokosuka Electrical Communication Laboratories, Nippon Telegraph and Telephone Public Corporation, Yokosuka, 238-03 Japan.

[1]Since the circuit utilizes the both substrate surfaces, let us call it the two-sided MIC.

0018-9480/82/0200-0227$00.75 ©1982 IEEE

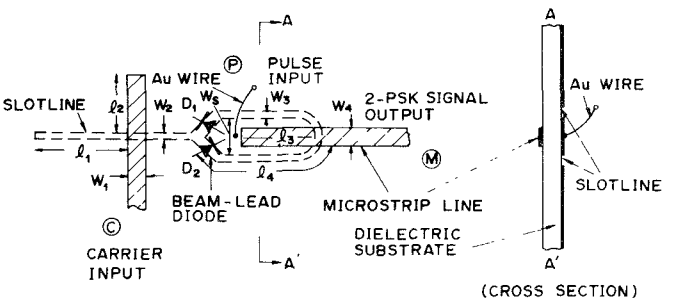

Fig. 1. Configuration of BPSK balanced modulator. Solid lines show microstrip lines on the substrate, dotted lines show slot lines on the reverse side of the substrate: $w_1 = w_4 = 0.3$ mm, $w_2 = w_3 = 0.06$ mm, $w_5 = 0.6$ mm, $l_1 = l_4 = 1.34$ mm, and $l_2 = l_3 = 1.1$ mm.

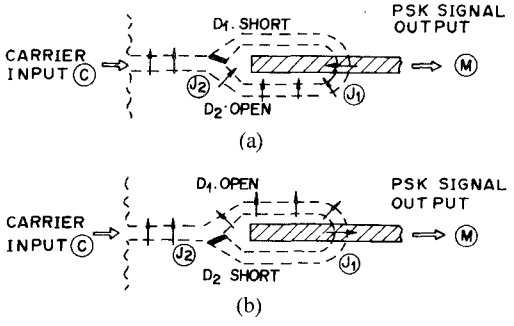

Fig. 2. Principle of BPSK modulation. Arrows represent the direction of electric field of carrier. (a) Positive pulse is supplied to diodes Diode D_1 is forward-biased (short), and diode D_2 is reverse-biased (open). (b) Negative pulse is supplied to diodes. Diode D_1 is reverse-biased (open), and diode D_2 is forward-biased (short).

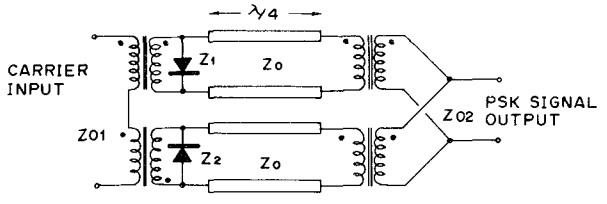

Fig 3 An equivalent circuit of BPSK balanced modulator. Quarter-wavelength distributed constant lines show slot lines.

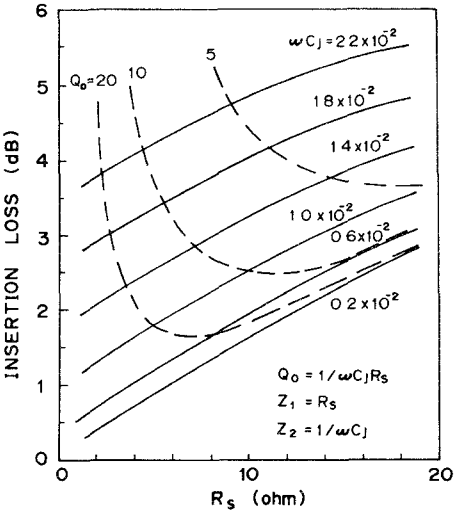

Fig. 4. Calculated insertion loss of the modulator. R_s is a series resistance and C_j is a junction capacitance The calculation conditions are as follows: $Z_{01} = 100$, $Z_{02} = 50$, $Z_0 = 70.7$, and $\theta = \pi/2$.

cylindrical conductors, which connect microstrip lines and slot lines, to supply modulating pulses and carriers to the diodes. Therefore, the realizable frequency of the modulator was limited to the frequencies up to the C-band. On the other hand, in the modulator shown in Fig. 1, the modulating pulse and the carrier are separately supplied to the diodes. The modulating pulse is supplied to the diodes by the Au wire, and the carrier is supplied to the diodes along the slot line. The modulated carrier is transmitted to the microstrip line by the slot-to-microstrip transition composed of an open-circuited quarter-wavelength microstrip line. The configuration of the modulator is suitable for planar circuits at high frequencies.

Fig. 2 shows the fundamental operation of the BPSK modulator. In this figure, arrows represent the schematic expression of the carrier, i.e., the arrows show the direction of the electric field of the carrier which propagates along the slot line. Fig. 2(a) and (b) show the case where the positive and the negative pulses are supplied to the diodes, respectively. The carrier is supplied to port C, and passes through each slot line according to the polarity of the modulating pulse. Then the carrier is fed to the microstrip line through the slot-to-microstrip transition. The direction of the electric field at junction J_1 is 180° out-of-phase for Fig. 2(a) and (b). Thus a BPSK modulated carrier is obtained from port M.

B. Modulation Loss Calculation

The equivalent circuit of the BPSK balanced modulator is shown in Fig. 3. Slot lines are expressed as distributed-constant lines. The junctions J_1 and J_2 are expressed by an ideal transformer. This type of circuit is a series-parallel connected circuit. Therefore, from the viewpoint of the equivalent circuit, it is a single-balanced modulator. Z_1 and Z_2 represent the diode impedance under the forward- and reverse-biased conditions. The Au wire, which supplies the modulating pulse, is omitted in Fig. 3, since it is isolated from the RF circuit, due to its series inductance and the concentration of the RF electromagnetic field on the slot line. The inductance behaves as a low-pass filter. The diode impedances Z_1 and Z_2 can be approximated to the series resistance R_s and the reactance $1/j\omega C_j$, respectively. C_j

TABLE I
ELECTRICAL CHARACTERISTICS OF DIODE (V558)

Parameter	Values
Series resistance	2.5 ohm
Junction capacitance at 0 Volt	0.05 pF
Breakdown voltage at 10 μm	5 volt
Forward voltage at 20 mA	0.8 volt
Ideality factor	1.17
Size	0.2 x 0.75 mm^2

corresponds to the junction capacitance of the diode. Since the real part of Z_2 is much smaller than the imaginary part, Z_2 is assumed to be an imaginary number.

The calculated insertion loss of the balanced modulator is shown in Fig. 4. Dotted lines show the insertion loss using the quality factor $Q_0 = 1/\omega C_j R_s$ [16]. The derivation of the equations is shown in detail in the Appendix. The calculation conditions are as follows: $Z_{01} = 100$, $Z_{02} = 50$, $Z_0 = 70.7$, and $\theta = \pi/2$. The insertion loss increases with an increase in the resistance and the capacitance of the diode.

C. Experimental Results

The BPSK balanced modulator has been fabricated by conventional photolithographic techniques on a 0.3-mm thick alumina substrate with a relative permittivity of 9.6. Nickel–chromium with a 500-Å thickness and gold with a 6000-Å thickness are deposited on the alumina substrate by the vacuum evaporation method. The thickness of the gold on the microstrip lines and slot lines is increased to about 4 μm by electroplating. The input impedance of the modulator is 50 Ω, and the impedance of the quarter-wavelegnth slot line is 70.7 Ω. The Au wire has a 50-μm diameter. It is connected to the pattern by thermal bonding. Diodes used in the modulator are beam-lead Schottky-barrier diodes (V558 of NEC). The typical characteristics of the diode are shown in Table I. In this experiment, the ridged waveguide [17] is used to construct the waveguide-to-microstrip transition. These transitions are connected to the carrier input port C and the BPSK modulated carrier output port M. A coaxial connector is used for supplying modulating pulses to the modulator.

The static performance of the BPSK modulator is shown in Figs. 5, 6, and 7. The insertion loss versus carrier input power characteristics for different diode bias currents are shown in Fig. 5. The carrier frequency is 27 GHz. When the carrier input power is greater than 10 dBm, the insertion loss increases with the increasing carrier input power. The insertion loss decreases with an increase in the forward current. The relationship between the insertion loss and the forward current of the diode is shown in Fig. 5(b). The insertion loss is 2.2 dB at a carrier input power of 5 dBm and a forward current of 20 mA.

Since two diodes are connected in antiparallel in the

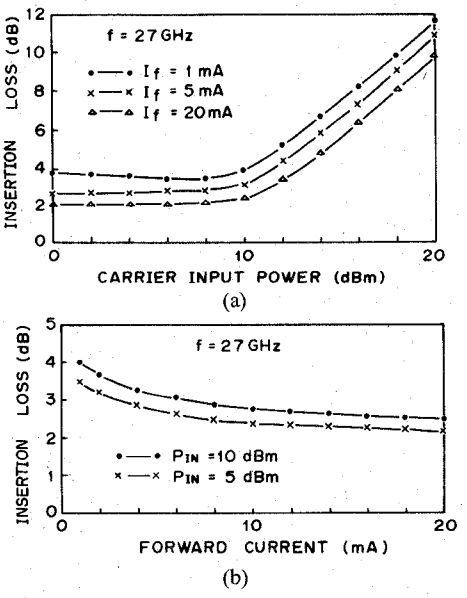

Fig. 5. (a) Measured insertion loss versus carrier input power. (b) Measured insertion loss versus forward current. The carrier frequency is 27 GHz.

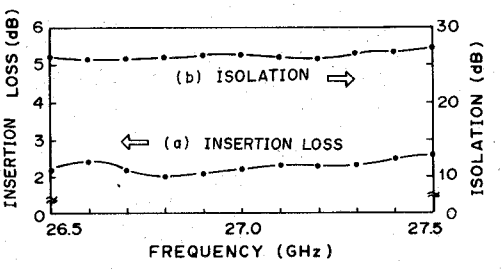

Fig. 6. Frequency response of BPSK modulator. (*a*) Insertion loss at a carrier input power of 5 dBm and a forward current of 20 mA. (*b*) Isolation between port C and port M.

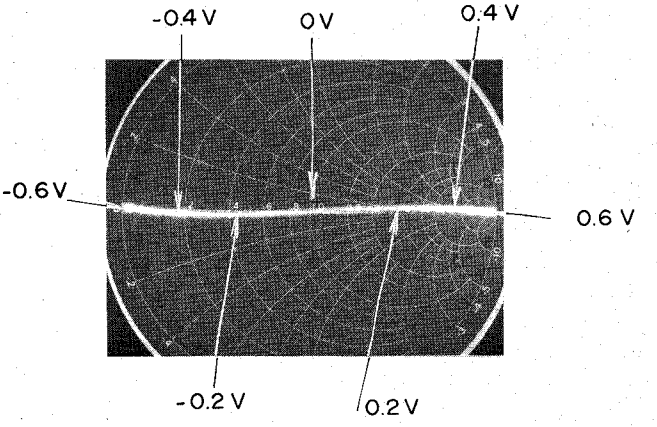

Fig. 7. Transient vector locus of BPSK modulator. The carrier frequency is 27 GHz. The carrier input power is 10 dBm. The applied voltage is +0.6 V to −0.6 V.

modulator (See Fig. 1), the handling-power capability of the modulator is restricted by the forward voltage (or current) of the diode. As the carrier input power increases, the impedance of the reverse-biased diode decreases due to the RF-voltage swing, and thereby the reflection of the input carrier increases. In other words, the handling-power

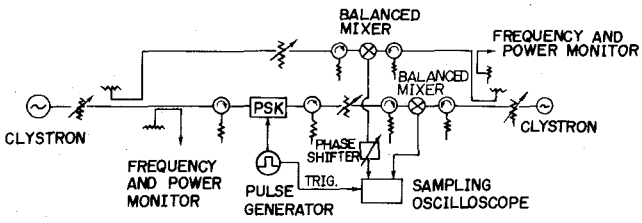

Fig. 8. Schematic diagram of the measurement setup.

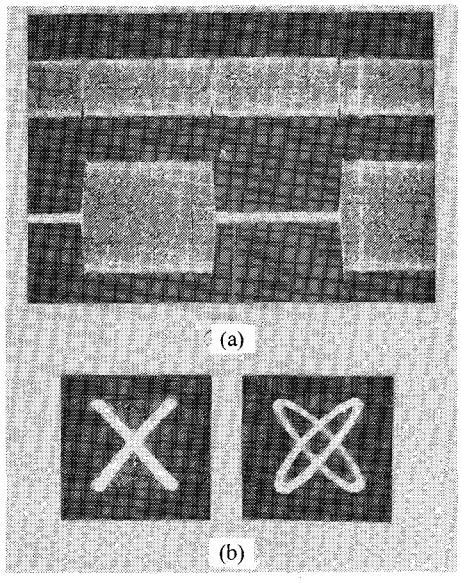

Fig. 9. Dynamic characteristics of BPSK modulator. The carrier frequency is 27 GHz and the modulating-pulse signal frequency is 30 MHz. The carrier input power is 10 dBm. (a) BPSK signal envelope and coherent detected waveforms (10 ns/div). (b) Lissajou figures.

capability depends upon the diffusion voltage of the Schottky-barrier diode (SBD). From this point, GaAs (diffusion potential $\doteqdot 0.8$ V) is better than S_i (diffusion potential $\doteqdot 0.6$ V). For S_i SBD, the handling-power capability was 4 dB lower than that for GaAs SBD [18].

From Fig. 4, the insertion loss of the modulator is estimated to be 1.1 dB since the diode used here has $R_s = 2.5$ and $\omega C_j = 0.008$. The insertion loss of the slot-to-microstrip transition is 0.3 dB at 27 GHz. The remaining 0.5 dB is considered to be conductor loss of the microstrip lines and slot lines, and reflection loss due to discontinuities.

Fig. 6 shows the frequency response of the insertion loss and the isolation between ports C and M. The loss variation is less than ± 0.3 dB for a frequency range of 26.5–27.5 GHz. The carrier input power and the forward current are fixed at 5 dBm and 20 mA, respectively. The isolation between the carrier input port and the modulated carrier output port is greater than 25 dB over a 1-GHz bandwidth.

The transient vector locus of the modulator is shown in Fig. 7. The phase error is less than 1°. The transient vector locus has a very little orthogonal component. The amplitude deviation is less than 0.5 dB.

The phase error is caused by the asymmetry of the two slot-line arms. Since the modulator uses both sides of the substrate, the asymmetry is due to the positioning error when the circuit pattern on both sides is made. However, in this case, no adjustment is required, since a phase error of less than 1° does not affect the C/N ratio degradation in digital communications [19].

The dynamic performance is measured by the setup shown in Fig. 8. The modulated carrier is converted by mixers to an intermediate frequency band of 1.7 GHz, and then the waveforms are measured with a sampling oscilloscope. The bandwidth of the measurement system is greater than 3 GHz. The carrier frequency is 27 GHz, and the modulating-pulse signal frequency is 30 MHz. The BPSK signal envelope and the coherent detected waveform are shown in Fig. 9(a). Fig. 9(b) shows the Lissajous figures. The rise time and fall time of the envelope waveform are less than 300 ps. Since the rise time and fall time of the modulating-pulse waveform are of the order of 200 ps, the modulator shows no transient characteristic degradation. The driver is the pulse generator TR-4200.[2] As a result the BPSK balanced modulator with good performance has been achieved in the 27-GHz band. This modulator is suitable for modulating carriers with medium power levels,

[2] Takeda Riken industry's limit.

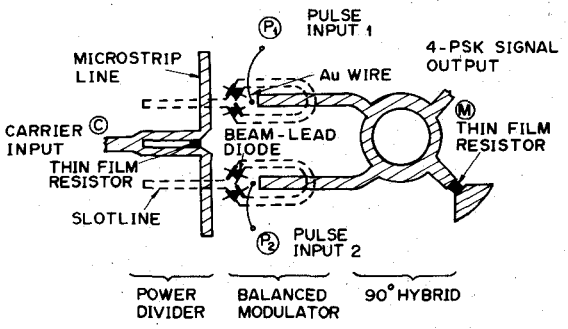

Fig. 10. Configuration of QPSK modulator. Solid lines show microstrip lines on the substrate, dotted lines show slot lines on the reverse side of the substrate.

and for constructing direct radio-frequency (RF) modulators followed by transmitting high-power amplifiers.

III. QPSK Balanced Modulator

A. Circuit Configuration

The configuration of the QPSK modulator, consisting of two BPSK modulators, a power divider, and a branch-line hybrid coupler is shown in Fig. 10. In this figure, solid lines indicate microstrip lines on the substrate, while dotted lines indicate slot lines on the reverse side of the substrate. C, M, P_1, and P_2 denote the carrier input port, the QPSK modulated carrier output port, and the modulating pulse input ports 1 and 2, respectively. The power divider splits the carrier supplied at port C, and two divided carriers are fed in-phase into two BPSK modulators. Two BPSK modulated carriers are combined with a 3-dB branch-line hybrid coupler to obtain a QPSK modulated carrier from port M.

The QPSK balanced modulator shown in Fig. 10 is made on a 0.3-mm thick alumina substrate fabricated by conventional photolithographic techniques. Since the power divider and the branch-line hybrid coupler require resistors, tantalum nitride (Ta_2N) resistors are sputtered on the alumina substrate. The construction of the metal layers on the substrate is a three-layer metal system, i.e., Ta_2N–NiCr–Au, while that on the reverse side of the substrate is a two-layer metal system, i.e., NiCr–Au. The sheet resistance of tantalum nitride is 35 Ω/square.

Fig. 11 shows photographs of the modulator pattern. The pattern of the microstrip lines on the substrate is shown in Fig. 11(a), and the pattern of the slot lines, on which beam-lead Schottky-barrier diodes are bonded, is shown in Fig. 11(b). In this experiment, the waveguide-to-microstrip transitions are connected to ports C and M. Fig. 11(c) shows a photograph of the modulator mounted in a test housing. The coaxial connectors are connected to ports P_1 and P_2. The microstrip pattern can be seen in the photograph.

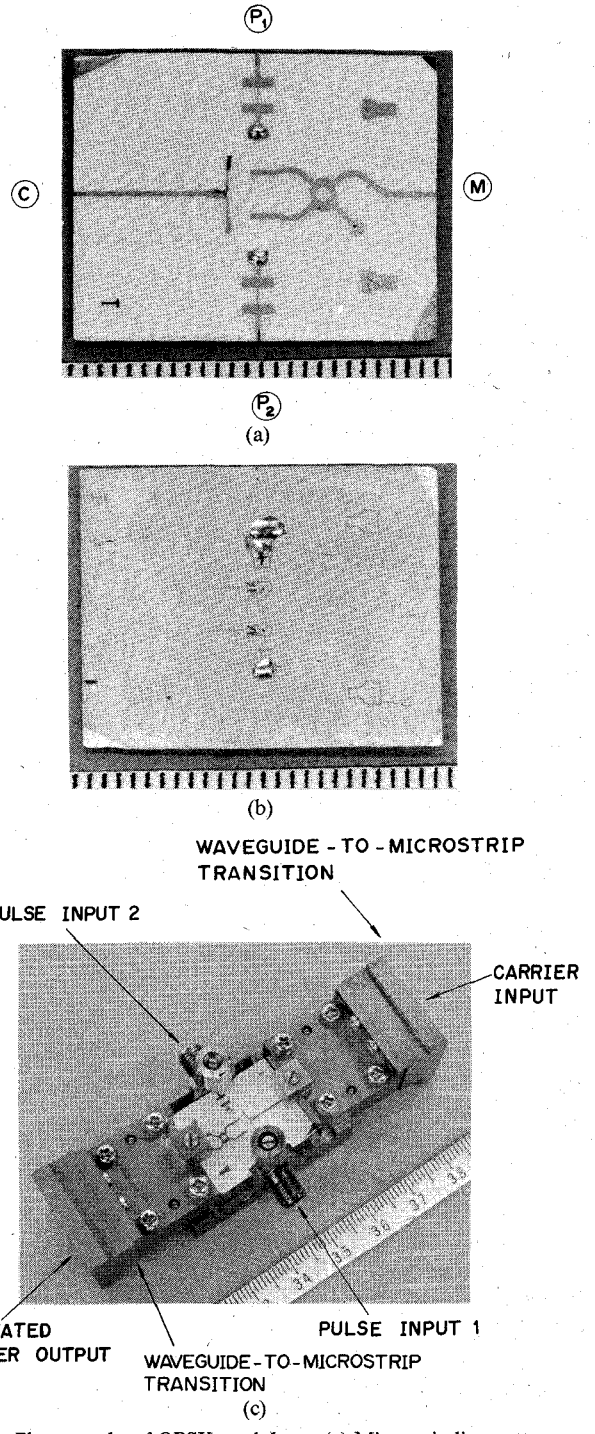

Fig. 11. Photographs of QPSK modulator. (a) Microstrip line pattern on the substrate (1 mm/div). (b) Slot line pattern on the reverse surface (1 mm/div). (c) QPSK modulator mounted in a test housing.

B. Experimental Results

The static performance of the QPSK modulator are shown in Figs. 12 and 13. The insertion loss versus carrier input power and the insertion loss versus forward current are shown in Fig. 12. The carrier frequency is fixed at 27 GHz. The insertion loss is constant up to a carrier input power of 13 dBm, because the QPSK modulator uses the two BPSK modulators whose features are described in Section II. The insertion loss is 6.3 dB at a carrier input power of 10 dBm and a forward current of 20 mA. Fig. 12(b) shows the insertion loss as a function of the forward current supplied to the diode. A forward current of 10 mA

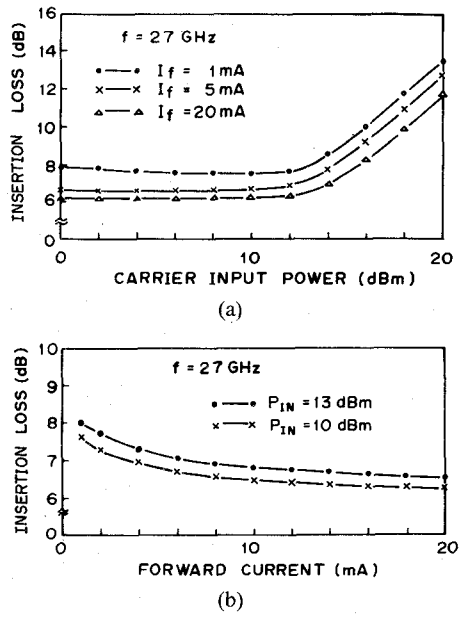

Fig. 12. (a) Measured insertion loss versus carrier input power. (b) Measured insertion loss versus forward current. The carrier frequency is 27 GHz.

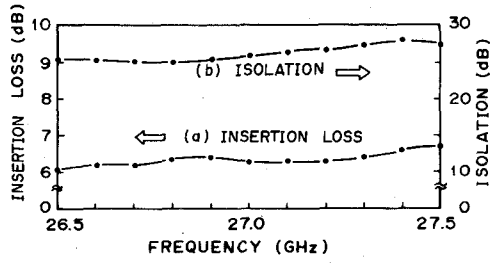

Fig. 13. Frequency response of QPSK modulator. (a) Insertion loss at a carrier input power of 10 dBm and a forward current of 20 mA. (b) Isolation between port C and port M.

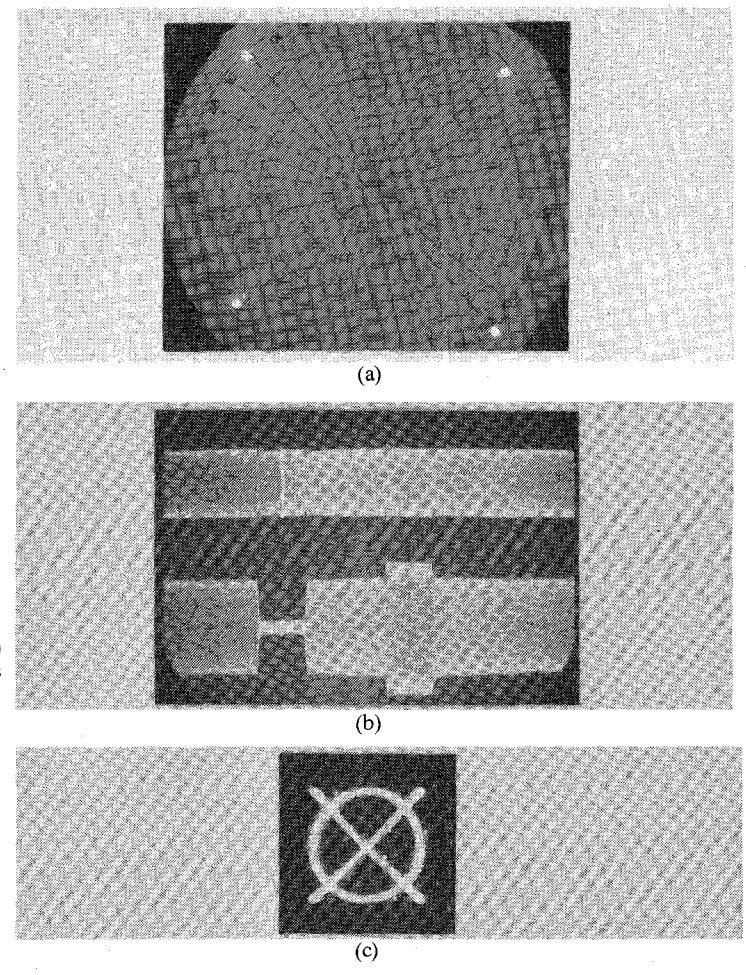

Fig. 14. Dynamic characteristics of QPSK modulator. The carrier frequency is 27 GHz and the modulating-pulse signal frequency is 30 MHz. The carrier input power is 13 dBm. (a) Four phase states of QPSK modulator. (b) QPSK signal envelope and coherent detected waveforms (10 ns/div). (c) Lissajou figure.

is sufficient to modulate the carrier at a power level of 13 dBm.

The insertion loss of 6.3 dB is alloted as follows: the intrinsic loss of the 3-dB branch-line hybrid coupler is 3 dB; the loss of the BPSK modulator is 2.2 dB at a carrier input power of 7 dBm; and the insertion loss of the power divider and the branch-line hybrid circuit are 0.6 dB and 0.5 dB, respectively.

The frequency response of the insertion loss and the isolation between ports C and M is shown in Fig. 13. The carrier input power and the forward current are fixed at 10 dBm and 20 mA, respectively. The minimum insertion loss is 6.1 dB at a carrier frequency of 26.5 GHz. The loss variation is less than ± 0.3 dB for a frequency range of 26.5–27.5 GHz. The isolation is greater than 25 dB over a 1-GHz bandwidth. The four phase states are shown in Fig. 14(a). The phase error is less than 2°. The phase error also includes that of the power divider and the branch-line hybrid coupler, therefore the phase error of the QPSK modulator is somewhat greater than that of the BPSK modulator. However the phase error realized here is small, and it does not affect the C/N ratio degradation in digital communications [19].

The dynamic performance is shown in Fig. 14(b) and (c). The carrier frequency is 27 GHz, and the modulating-pulse signal frequency is 30 MHz. The QPSK signal envelope and the coherent detected waveform are shown in Fig. 14(b). Fig. 14(c) shows the Lissajous figure. The rise time and fall time of the envelope waveform are less than 300 ps. As a result, the QPSK balanced modulator with small insertion loss and phase error, fast switching time, and high isolation has been achieved at the 27-GHz band.

IV. Conclusion

New MIC BPSK and QPSK balanced modulators have been fabricated at the 27-GHz band. These modulators utilize both substrate surfaces and employ slot lines and microstrip lines. The pulse input circuit is realized by a simple Au-wire bonding. The modulators use two Schottky-barrier diode (BPSK) or four diodes (QPSK).

The insertion loss for BPSK modulator is 2.2 dB at a carrier frequency of 27 GHz, and the isolation is greater than 25 dB over a 1-GHz bandwidth. The phase error and the amplitude deviation are less than 1° and 0.5 dB, respectively.

The QPSK modulator consists of two BPSK modulators,

a power divider, and a branch-line hybrid circuit. The insertion loss is less than 6.7 dB over a 1-GHz bandwidth. The isolation is greater than 25 dB. The phase error is less than 2°, and the rise time and fall time are less than 300 ps.

The modulator described in this paper can easily be extended to the millimeter-wave band up to 40–50 GHz. Furthermore, the integrated circuits of the BPSK and QPSK modulators are useful in constructing MIC transmitters in radio transmission systems. These modulators will enable compact, low-cost, and high-efficiency transmitters.

APPENDIX

Fig. 15 shows a schematic expression of a series-parallel connected circuit. Transfer matrices $[F_1]$ and $[F_2]$ are derived from the transfer matrices of the distributed-constant line, two ideal transformers, and the parallel-connected diode. Matrices $[F_1]$ and $[F_2]$ are expressed as follows:

$$[F_1]=\begin{bmatrix} A_1 & B_1 \\ C_1 & D_1 \end{bmatrix} = \begin{bmatrix} \cos\theta & jZ_0\sin\theta \\ Y_1\cos\theta + j\dfrac{1}{Z_0}\sin\theta & jY_1Z_0\sin\theta+\cos\theta \end{bmatrix} \tag{1}$$

$$[F_2]=\begin{bmatrix} A_2 & B_2 \\ C_2 & D_2 \end{bmatrix} = \begin{bmatrix} -\cos\theta & -jZ_0\sin\theta \\ -Y_2\cos\theta - j\dfrac{1}{Z_0}\sin\theta & -jY_2Z_2\sin\theta-\cos\theta \end{bmatrix} \tag{2}$$

where

$Y_1=1/Z_1$ forward-biased diode admittance;
$Y_2=1/Z_2$ reverse-biased diode admittance;
Z_0 characteristic impedance of the quarter-wavelength slot line;
θ electrical legnth of the quarter-wavelength slot line.

In (1) and (2), we assume that the distributed-constant line is lossless. From (1) and (2), the overall transfer matrix, $[F_T]$, of Fig. 15 is expressed as follows [20]:

$$[F_T]=\begin{bmatrix} A & B \\ C & D \end{bmatrix} = \frac{1}{D_1+D_2} \cdot \begin{bmatrix} 2+(A_1D_2+A_2D_1+B_1C_2+B_2C_1) & B_1D_2+B_2D_1 \\ C_1D_2+C_2D_1 & D_1D_2 \end{bmatrix}. \tag{3}$$

From (3), the transmission coefficient T_C is expressed as follows:

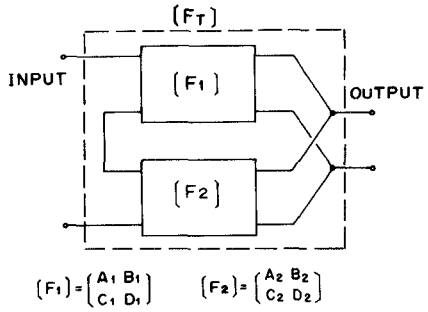

Fig. 15. Schematic expression of series-parallel connected circuit.

$$T_C=\frac{2\sqrt{Z_{01}Z_{02}}}{Z_{02}A+B+Z_{01}Z_{02}C+Z_{01}D} \tag{4}$$

where Z_{01} and Z_{02} are the input impedance of the circuit. Since the carrier input port and the PSK signal output port are connected to the diodes in series and in parallel, respectively, Z_{01} is set to $2Z_{02}$. From (3) and (4), the insertion loss of the modulator can be calculated. In the calculation, Z_1 and Z_2 are equal to R_s and $1/j\omega C_j$, respectively.

ACKNOWLEDGMENT

The authors wish to thank Dr. H. Yamamoto in the Yokosuka Electrical Communication Laboratory for his encouragement and suggestions.

REFERENCES

[1] T. Matsumoto and M. Aikawa, "A high-speed balanced modulator composed of slot lines," *Electron. Commun. Jap.*, vol. J60-B, pp. 350–357, May 1977.
[2] M. Aikawa and H. Ogawa, "2 GB double-balanced PSK modulator using coplanar waveguides," in 1979 *ISSCC Dig. Tech. Pap.* Feb. 1979, pp. 172–173.
[3] K. Miyauchi, S. Seki, and K. Yanagimoto, "Strip-line high-speed switches and modulators in the 4-GHz region," in *Proc. European Microwave Conf*, Sept. 1969, p. 119.
[4] Y. Itoh, H. Yunoki, H. Komizo, and J. Dodo, "*K*-band integrated microstrip modulator and mixer in waveguide for a high-speed PCM radio repeater," in 1972 *ISSCC Dig. Tech. Pap.*, Feb. 1972 pp. 160–161.
[5] J. M. Robinson and A. Husain, "Design of direct phase modulators for high speed digital radio systems using MIC techniques," in 1977 *IEEE MTT Int. Microwave Symp. Dig. Tech. Pap.*, June 1977, pp. 220–223.
[6] K. Miyauchi, S. Seki, and K. Yanagimoto, "Gigabit 4-phase modulation-demodulation circuits for microwave digital systems," in 1979 *IEEE MTT Int. Microwave Symp. Dig. Tech. Pap.*, May 1979, pp. 531–533.
[7] R. S. Caruthers, "Copper oxide modulators in carrier telephone systems," *Bell Syst. Tech. J.*, vol. 18, pp. 315–337. Apr. 1939.
[8] R. B. Mouw, "A broad-band hybrid junction and application to the star modulator," *IEEE Trans. Microwave Theory Tech.*, vol. MTT-16, pp. 911–918, Nov. 1968.
[9] M. Aikawa and H. Ogawa, "C band MIC double-balanced modulator for 2 Gbit/s PSK," in 1979 *ISCAS Dig. Tech. Papers*, July 1979, pp. 818–821.
[10] W. J. Clemetson, N. D. Kenyon, K. Kurokawa, B. Owen, and W. O. Schlosser, "An experimental mm-wave path length modulator," *Bell Syst. Tech. J.*, vol. 50, pp. 2917–2945, Nov. 1971.
[11] H. Yamamoto, K. Kohiyama, and K. Morita, "400-Mb/s QPSK repeater for 20-GHz digital radio-relay system," *IEEE Trans. Microwave Theory Tech.*, vol. MTT-23, pp. 334–341, Apr. 1975.
[12] H. Junghans, "A *Ku*-band hybrid-coupled 4-phase modulator in

MIC technology," in *Proc. 5th European Microwave Conf.*, Sept. 1975, pp. 133–137.
[13] B. Glance and N. Amitay, "A fast-switching low-loss 12-GHz microstrip QPSK path length modulator," *IEEE Trans. Commun.*, vol. COM-28, pp. 1824–1828, Oct. 1980.
[14] Yu-Wen Chang, H. J. Kuno, and D. L. English, "High data-rate solid-state millimeter-wave transmitter module," *IEEE Trans. Microwave Theory Tech.*, vol. MTT-23, pp. 470–477, June 1975.
[15] C. L. Cuccia and E. W. Matthews, "PSK and QPSK modulators for gigabit data rates," in 1977 *IEEE MTT Int. Microwave Symp. Digest Tech. Papers*, June 1977, pp. 208–211.
[16] K. Kurokawa and W. O. Schlosser, "Quality factor of switching diodes for digital modulation," *Proc. IEEE*, vol. 58, pp. 180–181, Jan. 1970.
[17] S. Hopfer, "The design of ridged waveguide," *IRE Trans. Microwave Theory Tech.*, vol. MTT-3, pp. 20–29, Oct. 1955.
[18] H. Ogawa and M. Aikawa, "An experimental investigation of 27-GHz band integrated PSK modulator," *Tech. Group Microwaves, IECE Japan*, MW-79-78, Oct. 1979.
[19] H. Yamamoto, K. Morita, and S. Komaki, "Error rate performance of QCPSK system with various degradation factors," *Electron. Commun. Japan*, vol. 58-B, pp. 584–591, Nov. 1975.
[20] R. Sato, *Transmission Circuit*. Tokyo: Corona, 1973, pp. 43–47.

✤

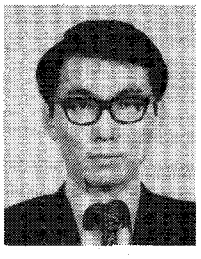

Hiroyo Ogawa was born in Sapporo, Japan, in 1951. He received the B.S. and M.S. degrees in electrical engineering from Hokkaido University, Sapporo, Japan, in 1974 and 1976, respectively.

He joined Yokosuka Electrical Communication Laboratories, Nippon Telegraph and Telephone Public Corporation, Yokosuka, Japan, in 1976, and has been engaged in the research of microwave integrated circuits. He is presently engaged in the research of millimeter-wave integrated circuits.

Mr. Ogawa is a member of the Institute of Electronics and Communication Engineers of Japan.

Masayoshi Aikawa (M'74) was born in Saga, Japan, on October 16, 1946. He received the B.S. and M.S. degrees in electrical engineering from the Kyushu University, Fukuoka, Japan, in 1969 and 1971, respectively.

He joined the Electrical Communication Laboratory, Nippon Telegraph and Telephone (NTT) Public Corporation, Tokyo, Japan, in 1971, and has since been engaged in researching and developing microwave-integrated-circuits for radio communication systems. He is now a assistant chief of the Radio Transmission Section in Yokosuka Electrical Communication Laboratory, NTT Public Corporation, Yokosuka, Japan.

Mr. Aikawa is a member of the Institute of Electronics and Communication Engineers of Japan.

✤

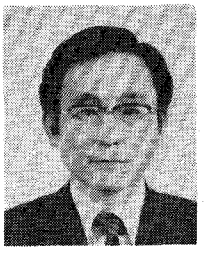

Masami Akaike (S'65–M'76) was born in Kamakura-shi, Kanagawa-ken, Japan, on October 15, 1940. He received the B.S., M.S., and Ph.D. degrees from the University of Tokyo, Tokyo, Japan, in 1964, 1966, and 1969, respectively.

He joined the Musashino Electrical Communication Laboratory, Nippon Telegraph and Telephone Public Corporation, Tokyo, Japan, in 1969. He was engaged in the research of millimeter-wave solid-state circuits and the development and design of repeaters and measuring equipments for a guided millimeter-wave transmission system. He is currently a Staff Engineer of the Radio Transmission Section, Trunk Transmission System Development Division, Yokosuka Electrical Communication Laboratory, NTT.

Dr. Akaike is a member of Japan, and was a recipient of the 1971 IECEJ Yomezawa Memorial Scholarship.